

# Fuel Economy Analysis of Part-Load Variable Camshaft Timing Strategies in Two Modern Small-Capacity Spark Ignition Engines

Bonatesta<sup>a,\*</sup>, F., Altamore<sup>a</sup>, G., Kalsi<sup>a</sup>, J., and Cary<sup>b</sup>, M.

<sup>a</sup> Oxford Brookes University, Department of Mechanical Engineering and Mathematical Science, Wheatley Campus, Oxford, OX33 1HX, UK

<sup>b</sup> Ford Motor Company, Dunton Technical Centre, Laindon, SS15 6EE, UK

**Keywords:** Variable Camshaft Timing, Variable Valve Timing, Down-sized engine, Cylinder Charge Dilution, Direct Injection, Fuel Economy

## Highlights

- Valve timing strategies are explored at part-load in two small-capacity SI engines
- Simplified graphical fuel-economy VCT strategies are provided for the two engines
- Engine design specifics exert a profound influence upon optimal valve timings
- The theoretical best strategy determines BSFC reduction above 8% for the PFI engine
- Maximum BSFC reduction was about 5% for the more efficient GDI platform

## ABSTRACT

Variable Camshaft Timing strategies have been investigated at part-load operating conditions in two 3-cylinder, 1.0-litre, Spark Ignition engines. The two small-size engines are different variants of the same 4-valve/cylinder, pent-roof design platform. The first engine is naturally aspirated, port fuel injection and features high nominal compression ratio of 12:1. The second one is the turbo-charged, direct injection version, featuring lower compression ratio of 10:1. The aim of the investigation has been to identify optimal camshaft timing strategies which maximise engine thermal efficiency through improvements in brake specific fuel consumption at fixed engine load.

The results of the investigation show that the two engines demonstrate consistent thermal efficiency response to valve timing changes in the low and mid part-load envelope, up to a load of 4 bar BMEP. At the lower engine loads investigated, reduced intake valve opening advance limits the hot burned gas internal recirculation, while increasingly retarded exhaust valve opening timing favours engine efficiency through greater effective expansion ratio. At mid load (4 bar BMEP), a degree of intake advance becomes beneficial, owing mostly to the associated intake de-throttling. In the upper part-load domain, for engine load of 5 bar BMEP and above, the differences between the two engines determine very different efficiency response to the valve timing setting. The lower compression ratio engine continues to benefit from advanced intake valve timing, with a moderate degree of exhaust timing retard, which minimises the exhaust blow-down losses. The higher compression ratio engine is knock-limited, forcing the valve timing strategy towards regions of lower intake advance and lower hot gas recirculation. The theoretical best valve timing strategy determined peak fuel economy improvements in excess of 8% for the port fuel injection engine; the peak improvement was 5% for the more efficient direct injection engine platform.

## 1. INTRODUCTION

In 2011, the International Energy Agency, in conjunction with the Global Fuel Economy Initiative, published a report which addresses their long term goal as a 50% reduction in global average emissions by the year 2030 [1]. Policy changes, enhanced technologies, revised fuels and reduced vehicle and engine size are indicated as possible ways to improving vehicles fuel economy, which in turn reduces pollutant emissions. In the last three decades, advanced technologies such as direct injection, turbo-charging and Variable Camshaft Timing (VCT), have contributed significantly to the evolution of engine design. Combinations of these technologies, along with engine down-sizing, have simultaneously delivered positive effects on fuel consumption and emissions [2, 3], as well as on driving pleasure [4].

Today's engine technical developments are primarily focused on improved part-load driving performance and fuel consumption with stoichiometric operation [5, 6]. One way of targeting these goals is through the implementation of VCT systems. The evaluation of the extent to which the VCT

\* Corresponding Author: Dr Fabrizio Bonatesta  
Email: [fbonatesta@brookes.ac.uk](mailto:fbonatesta@brookes.ac.uk)

60 technology impacts on fuel savings, especially within the framework of current down-sized engines, is  
61 of paramount importance. This evaluation, which enables the relative importance of the VCT system  
62 to be assessed, is the primary objective of the present study.

### 63 64 **1.1 Variable Camshaft Timing**

65 In engines with fixed camshaft timing, the exhaust valve is normally closed 15 to 30 Crank Angle (CA)  
66 degrees After Top Dead Centre (ATDC), whereas the intake valve is opened 10 to 20 CA degrees  
67 Before Top Dead Centre (BTDC). These timings represent a compromise between several functions,  
68 intended to provide sufficient valve overlap duration for good cylinder scavenging, but avoiding at the  
69 same time excessive backflow from the exhaust port. By contrast, the flexibility associated to the VCT  
70 technology has the potential to improve fuel economy, performance, as well as emission levels of  
71 gasoline engines over wide ranges of running conditions [7]. The advantage of wide valve overlap  
72 occurs especially at higher engine load and increasing engine speed, owing to improved volumetric  
73 efficiency. At low engine speed, wide overlaps are generally detrimental, yielding higher residual gas  
74 fraction [8] which may significantly degrade the combustion stability. Improvements in Brake Specific  
75 Fuel Consumption (BSFC) of up to 10%, as a result of early Intake Valve Opening (IVO) strategies,  
76 have been reported in recent studies [9, 10]; these explain the observed changes referring to the  
77 displacement of fresh mixture with residuals during valve overlap, ultimately reducing the *need for*  
78 *throttling* [6]. If the intake cam profile is fixed, the effects of IVO are inevitably linked to those of Intake  
79 Valve Closing (IVC) timing. Because of fresh mixture backflow at low engine speed, and inertia of the  
80 incoming gas flow at higher speed [11], the IVC timing shows significant effects on cylinder trapped  
81 mass, and hence on the resulting pumping (intake throttling) losses. Sizeable improvements in  
82 thermal efficiency have been observed with early IVC strategies, owing to greater effective  
83 compression ratio [12, 13].

84  
85 In traditional, fixed camshaft timing engines, the exhaust valve timing setting is a compromise  
86 between improved exhaust blow-down (achieved with early Exhaust Valve Opening, EVO) and  
87 greater work per cycle, associated to greater effective expansion ratio (late EVO). The influence of  
88 exhaust VCT on Internal Exhaust Gas Recirculation (I-EGR) is another very relevant factor. At part-  
89 load, the beneficial influence of late Exhaust Valve Closing (EVC) on cylinder scavenging, normally  
90 seen at high engine speed, tends to reduce; as speed and load are reduced, retarded EVC enables  
91 increasingly larger backflow from the exhaust to the intake system, which increases the fresh charge  
92 burned fraction. A similar though generally smaller effect is associated to early EVC taking place  
93 before Top Dead Centre (TDC), due to trapping large amounts of burned gases within the cylinder at  
94 the end of the exhaust stroke.

95  
96 As of today, the exhaust-only and intake-only variable camshaft timing schedules remain the most  
97 practical and cost-effective in use. Typically, at part-load running conditions, intake-only strategies  
98 entail significantly advanced intake valve timing and asymmetric valve overlaps extended well into the  
99 exhaust stroke. In terms of benefits on fuel consumption, Leone et Al. [14] found that due to increased  
100 charge dilution, a higher intake manifold pressure is required to maintain a given load, which in turn  
101 reduces the pumping work. Similar reasoning, along with increased expansion work, justifies the use  
102 of retarded exhaust valve timing at part-load, in the case of exhaust-only strategies. The Dual or Twin  
103 Independent VCT systems, where the two camshafts can be phased continuously and independently  
104 of one another, would synthesize the benefits of both exhaust and intake-only schedules; however,  
105 DI-VCT mechanisms are bulkier, more expensive and more complicated to operate. Kramer and  
106 Philips [15] found that, using a DI-VCT strategy, the fuel economy was improved due to the following  
107 three, concurrent phenomena: de-throttling due to late IVC (backflow of mixture into the intake  
108 manifold); de-throttling due to late EVC (internal Exhaust Gas Recirculation); increased effective  
109 expansion ratio due to late EVO (more work extracted in each engine cycle).

### 110 111 **1.2 Engine Down-sizing**

112 Internal combustion engine down-sizing is becoming increasingly common because of the inherent  
113 advantages of high specific power and torque, lower fuel consumption and emissions, as well as  
114 improved driveability [4, 16]. Due to lower displacement volume, the down-sized engine tends to work  
115 at higher load with reduced throttling/pumping losses [17]. The potential reduction in engine fuel  
116 consumption, averaged upon the New European Drive Cycle (NEDC), has been shown to increase  
117 exponentially with the factor of down-sizing [18]. High specific outputs are often achieved by means of  
118 turbo-charging. Currently, single-stage mechanical turbo-charging is the standard method, but more  
119 efficient systems such as multi-stage mechanical or electric super-chargers are being developed, with

sizeable improvements expected in torque output in the low engine speed range [16, 19]. Large low-end torque, which naturally leads to improved fuel economy, is a distinctive characteristic of down-sized gasoline engines featuring a combination of turbo-charger and VCT technologies [20].

Improvements of part-load specific fuel consumption from a turbo-charged gasoline engine with down-sizing factor of 40%, have been found to be of the order of 12% over the NEDC, when compared to a traditional naturally aspirated engine [21]. In the recent collaborative Ultra-Boost project, Turner et Al. [22] found that an extreme down-sizing factor of 60%, applied to a naturally aspirated, 8-cylinder engine, resulted in 23% reduction in part-load specific fuel consumption over the same drive-cycle. The purposely developed engine platform incorporated Direct Injection (DI), Variable Camshaft Timing and multi-stage forced induction technologies. The extent to which each single system contributed towards the overall fuel economy improvement of 23% was not reported.

One significant efficiency limitation of down-sized engines is the knock tendency, associated with high specific power output. Due to its marked effect on cylinder charge cooling, the introduction of fuel DI minimises the risk of knock, enabling the implementation of comparatively higher compression ratio, with measurable benefits in terms of engine thermal efficiency [23, 24]. Baêta et Al. [25] suggest the use of pure ethanol fuel in direct injection spark ignition engines may enable a *more aggressive* approach to down-sizing. The maximum part-load brake thermal efficiency recorded in their 1.4 litre twin-stage-compressor VCT prototype engine was 44%. Fuel direct injection also improves volumetric efficiency across all operating conditions, and this effect is amplified by parallel implementation of VCT technology. Shinagawa et Al. [20] have shown how the tuning of the exhaust valve timing and opening duration may lead to reduced exhaust gases blow-back pulsations, and hence improved volumetric efficiency at low speed.

The availability of advanced, fast-response VCT systems has in fact opened up several different potential avenues for improving the fuel economy of gasoline engines, including the implementation and/or optimisation of alternative engine cycles not viable until recently. Among others, the Miller cycle has potentials for improved fuel economy across a wide engine load range, both by reducing pumping work and mitigating knock tendency [26, 27]. Very early or very late intake valve closing timings can be used to control the amount of intake air, with a corresponding reduction of the effective compression ratio. Li et Al. [26] reported an 11% improvement in net Indicated Specific Fuel Consumption when early Miller cycle IVC timing was used at low speed and variable load between 4.5 and 9.0 bar IMEP. They suggest the optimisation of early IVC timing and intake cam profile brings a concrete prospect for further improvement of gasoline turbo-charged engines.

The present study is specifically concerned with the influence of Dual Independent Variable Camshaft Timing technology upon the fuel economy of modern small-size gasoline engines operating upon traditional spark ignition cycles. Of particular interest have been the complex relationships which establish between valve timing and BSFC, as the engine operating conditions are varied across relevant points of the part-load envelope. The importance of the present work lies in that it investigates and compares the results of two engine platforms of the same size and geometry, but featuring different injection technology and different compression ratio. While most recent studies [20, 21, 22] report overall efficiency gains from a range of combined technology, this work aims to explore the specific extent to which VCT technology can effectively improve the fuel economy of state-of-the-art gasoline engines. Importantly, in this evaluation process the limitations of current VCT technology remain identified. Another novelty of this work is that the comparison between the two engines unveils how the selection of the optimal valve timing is intimately correlated to the effects of compression ratio as well as those of fuel injection.

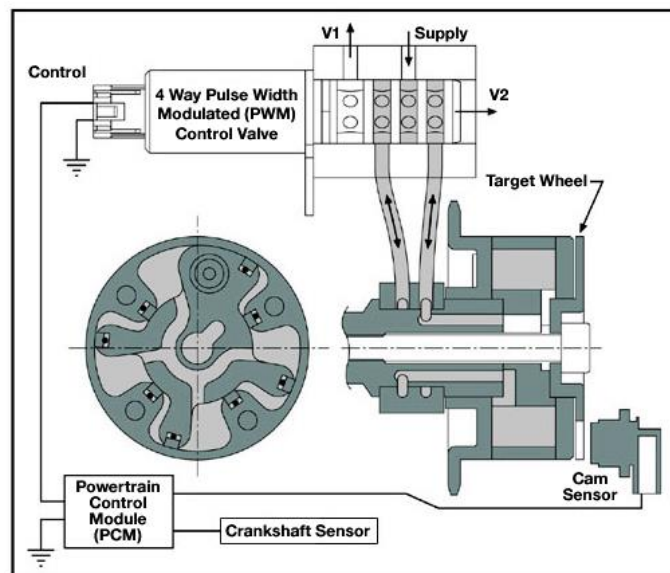
## 2. METHODOLOGY

Variable camshaft timing strategies for fuel economy are investigated in two modern small-capacity test engines. Test engine A is a naturally aspirated, port fuel injection, 1.0 litre, 3-cylinder, 4-stroke engine, with high nominal compression ratio of 12:1. Test engine B is the turbo-charged, direct-injection variant of the same engine, bearing a smaller nominal compression ratio of 10:1. According to the prevailing classification, engine B is a down-sized engine. The VCT mechanism used in test engine A allows independent intake and exhaust valve phase variation, whereas the valve lifting profiles remained fixed. The system allows phase variation over a range of 45 CA deg for both cams, with a resulting maximum valve overlap of 90 CA deg. The VCT mechanism used in test engine B is essentially the same; the only difference is a slightly shorter intake cam variability. The technical

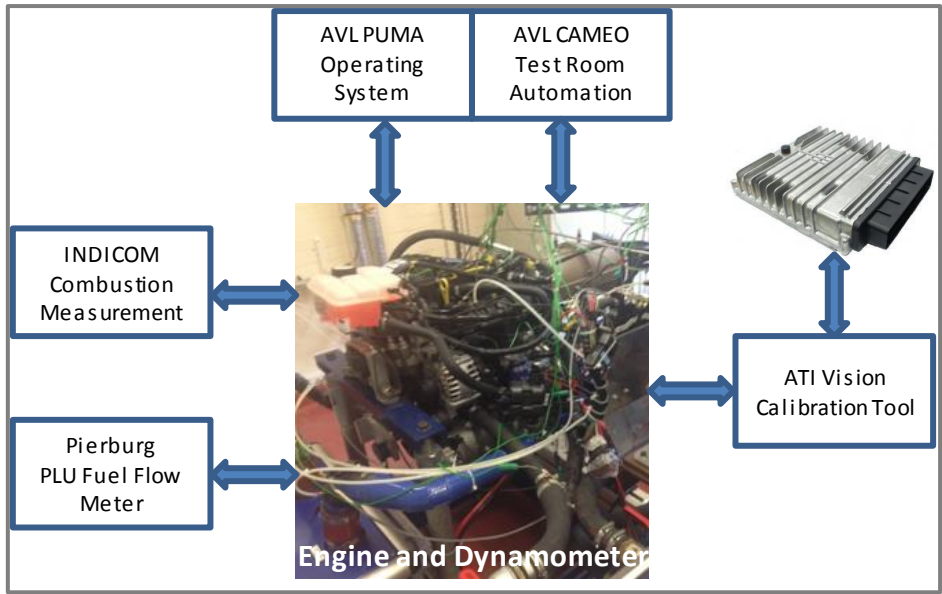
180 specifications of the two test engines and associated VCT system operation are given in Table 1. The  
 181 basic schematic of the variable cam phaser and its main components is presented in Figure 1 [28].  
 182 Figure 2 shows the schematic of the test room including engine and dynamometer assembly, test rig  
 183 control and data acquisition systems.  
 184

	Engine A	Engine B
<b>Total Displacement (cm<sup>3</sup>)</b>	999	999
<b>Stroke (mm)</b>	82	82
<b>Nominal Compression Ratio</b>	12:1	10:1
<b>Connecting Rod Length (mm)</b>	138.7	137
<b>Engine Type</b>	Naturally Aspirated, 3-Cylinder In-line, DOHC	Turbo Charged, 3-Cylinder In-line, DOHC
<b>Combustion Chamber</b>	4-Valve, Central Spark Plug, Pent-Roof Design	4-Valve, Central Spark Plug, Pent-Roof Design
<b>Engine Cycle</b>	4-Stroke Spark Ignition	4-Stroke Spark Ignition
<b>Fuel Injection System</b>	Port Fuel Injection	Direct Injection Common Rail; Centrally-Mounted Injector (Spray-Guided System)
<b>Test Programme Fuel</b>	E22 (78% Gasoline, 22% Ethanol by Volume)	95 RON Gasoline
<b>Maximum Rated Power</b>	62.5 kW at 6300 rev/min	88 kW at 6000 rev/min
<b>Maximum Rated Torque</b>	105 Nm at 4500 rev/min	170 Nm, 1500-4000 rev/min
<b>IVO Pin-Lock Position (CA deg ATDC)</b>	0 (TDC)	+ 5
<b>IVO Variability (CA deg)</b>	45	40
<b>Inlet Valve Opening Duration (CA deg)</b>	240	228
<b>EVC Pin-Lock Position (CA deg BTDC)</b>	0 (TDC)	0 (TDC)
<b>EVC Variability (CA deg)</b>	45	45
<b>Exhaust Valve Opening Duration (CA deg)</b>	236	228

185 Table 1. Technical specifications of test engines A and B  
 186

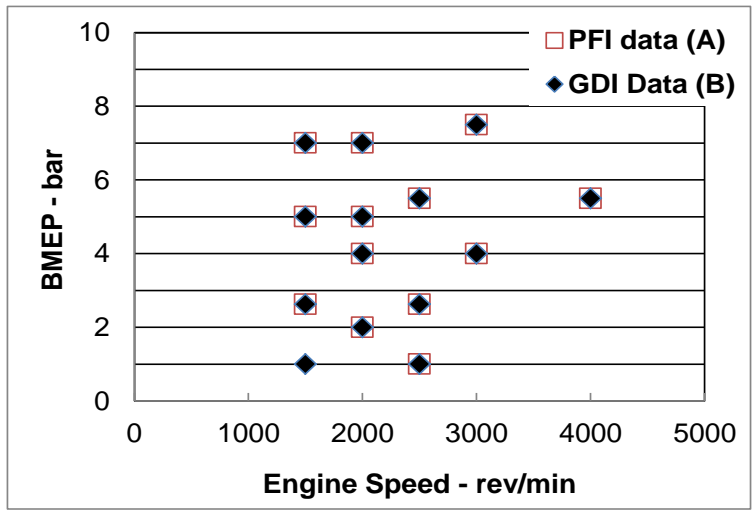


187 Figure 1. Variable cam phaser system used for intake and exhaust valve timing control; includes oil control valve, control  
 188 module, crank and cam sensors [24]  
 189



190  
191 **Figure 2.** Schematic of engine test room including rig control and data acquisition systems.  
192

193 The two engines were tested in steady-state conditions, over relevant portions of the part-load  
194 operating envelope, so as to represent typical urban and cruise driving conditions. As shown in Figure  
195 3, 13 speed and load combinations were selected for engine A, based on emissions and fuel  
196 economy residency information relevant to the NEDC and Federal Test Procedure (FTP) drive cycles  
197 [29]. For engine B, 14 points were selected. Engine speed and load were varied in the range 1500 to  
198 4000 rev/min, and in the range 1 to 7.5 bar Brake Mean Effective Pressure (BMEP), respectively. At  
199 each engine speed, dynamometer torque variation as a result of the VCT operation was annulled via  
200 throttle adjustment.  
201



202  
203 **Figure 3.** Part-load operating conditions investigated.  
204

205 Engine A was tested in stoichiometric conditions using E22 fuel blend (78/22 gasoline/ethanol volume  
206 ratio). The gasoline in the blend was pump-grade 95 RON fuel. The blend stoichiometric AFR was  
207 13.32. The proportion of oxygenate compounds, enabling the use of higher compression ratio, was  
208 dictated by the specific market destination for engine A. Engine B was also operated in stoichiometric  
209 conditions, employing early direct fuel injections in the intake stroke to ensure theoretically  
210 homogeneous cylinder gas mixture at the time of ignition. In this case, the fuel used was straight 95  
211 RON gasoline. The whole test programme for the two engines was carried out in fully-warm, steady-  
212 state conditions, and the ignition timing advance was adjusted to Maximum Brake Torque (MBT)  
213 timing for each speed and load combination. A MBT-Limited rule was applied to some higher load  
214 cases to avoid the inception of knock. Here, the ignition timing was retarded of 2 CA degrees from the  
215 location where knock was first detected. At each test point, fundamental cycle-average quantities  
216 were recorded to enable the VCT schedule optimisation. Improvements in thermal efficiency as a

217 result of the VCT operation were signalled via decreased Brake Specific Fuel Consumption. Parallel  
 218 measurements of CA-resolved in-cylinder pressure were taken on one cylinder to enable the analysis  
 219 of combustion and its variability. A Kistler 6125 piezo-electric pressure sensor was used to acquire in-  
 220 cylinder pressure data. The measurement resolution was variable: 0.2 CA degree during the rapid  
 221 burning angle; 1 CA degree along the remainder of the engine cycle [30]. In order to maximise the  
 222 beneficial effects of variable valve timing without compromising combustion stability and hence  
 223 vehicle driveability, the fuel economy optimisation process was conditioned to the Coefficient Of  
 224 Variability (COV) of Gross Mean Effective Pressure (GMEP) being always smaller or equal to 5% [31].  
 225

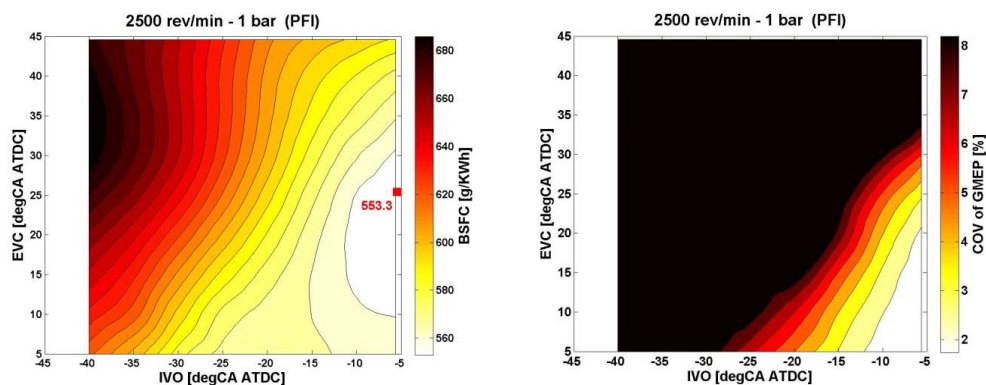
226 At each speed and load point, engine data were recorded at 5 CA degree regular increments of the  
 227 exhaust and intake valve timing, following a classic/uniform grid of points. The behaviour of the data  
 228 was summarised by using a cubic polynomial model, yielding response surfaces for ease of  
 229 visualisation. This approach carried the additional benefit of reducing the noise in the experimental  
 230 measurements [32, 33]. The full range of variability of intake and exhaust valve timing gave a 10x10  
 231 grid of points. Nevertheless, in some engine conditions smaller experimental grids were sufficient to  
 232 identify the optimal VCT setting for best thermal efficiency. This approach minimised the need for  
 233 testing, avoiding expensive experiments especially in regions of high cyclic variability.  
 234

### 235 3. RESULTS AND DISCUSSION

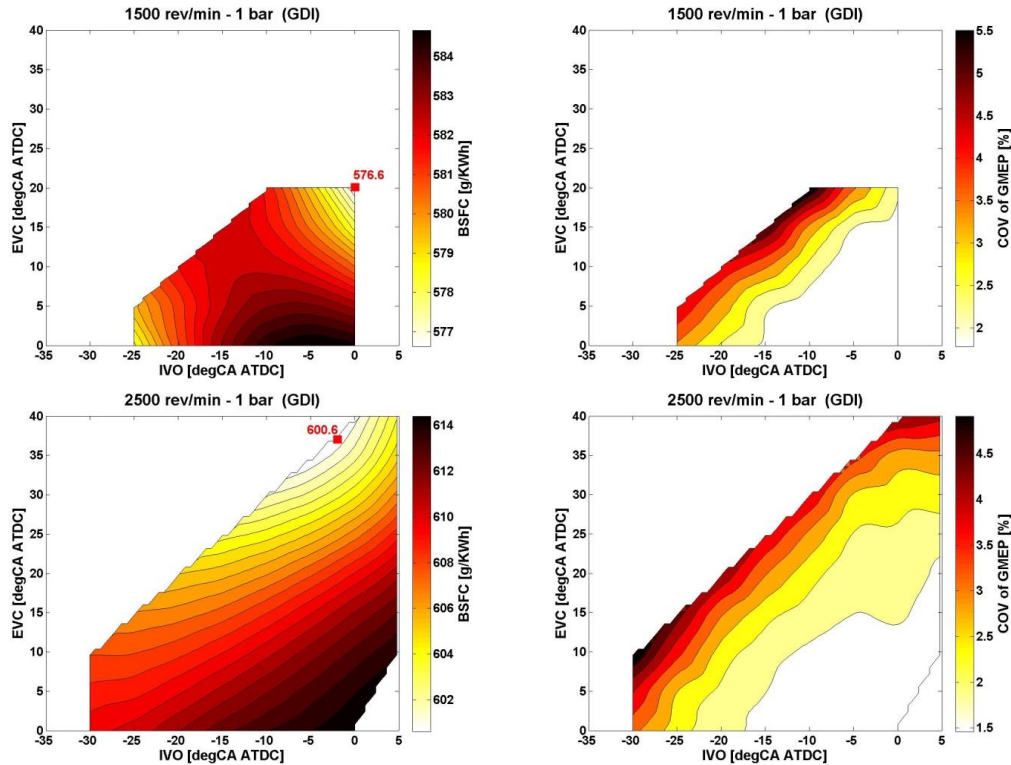
236 The experimental results regarding the BSFC response to variations of the intake and exhaust VCT  
 237 setting are presented and discussed in this section. Other experimental and calculated data such as  
 238 cycle-by-cycle variability, intake manifold pressure and CA location of 50% Mass Fraction Burned  
 239 (MFB50) are used to aid the discussion. Contour-plot type maps have been used for the analysis of  
 240 the BSFC response metrics. The experimental records of BSFC are interpolated, as described in  
 241 Section 2, over a uniform grid of IVO and EVC timing points. Same approach is used for the COV of  
 242 GMEP. For ease of visualisation, COV data above 8% have been given a single-colour pattern in the  
 243 relevant contour-plot maps. In the following sections, the results are conveniently arranged by fixed  
 244 engine load intervals and increasing engine speed.  
 245

#### 246 3.1 Influence of VCT setting in the low part-load region

247 Figures 4 and 5 show the BSFC and COV response metrics for the two test engines at a load of 1 bar  
 248 BMEP and increasing engine speed. For the PFI engine (engine A), only data at 2500 rev/min were  
 249 available. At the lowest speed and load investigated, the two engines show consistent response to  
 250 changes of the VCT setting, with minimum BSFC gained for late intake opening (close to TDC) and  
 251 limited degree of EVC retard (20 to 25 CA deg ATDC). As clearly suggested by the COV data, a  
 252 strong intake-to-exhaust pressure differential enables considerable internal burned gas recirculation  
 253 and high levels of cylinder charge dilution; virtually, any valve overlap duration in excess of 30 CA deg  
 254 results in degraded combustion and worsened fuel economy. As early IVO and late EVC are reported  
 255 to exert similar influence upon charge dilution at low engine load [6], the experimental data suggest  
 256 the effects of increased effective expansion ratio (more work extracted per cycle) would be more  
 257 significant than those associated to increased effective compression ratio. As the engine speed is  
 258 increased at low load for engine B (Figure 5), the overlap duration reduces in real time, limiting the  
 259 amount of internal recirculation; here combustion regains stability and further retarding the EVC timing  
 260 becomes beneficial. At 2500 rev/min, an EVC setting of 35 CA deg ATDC ensures minimum BSFC.  
 261



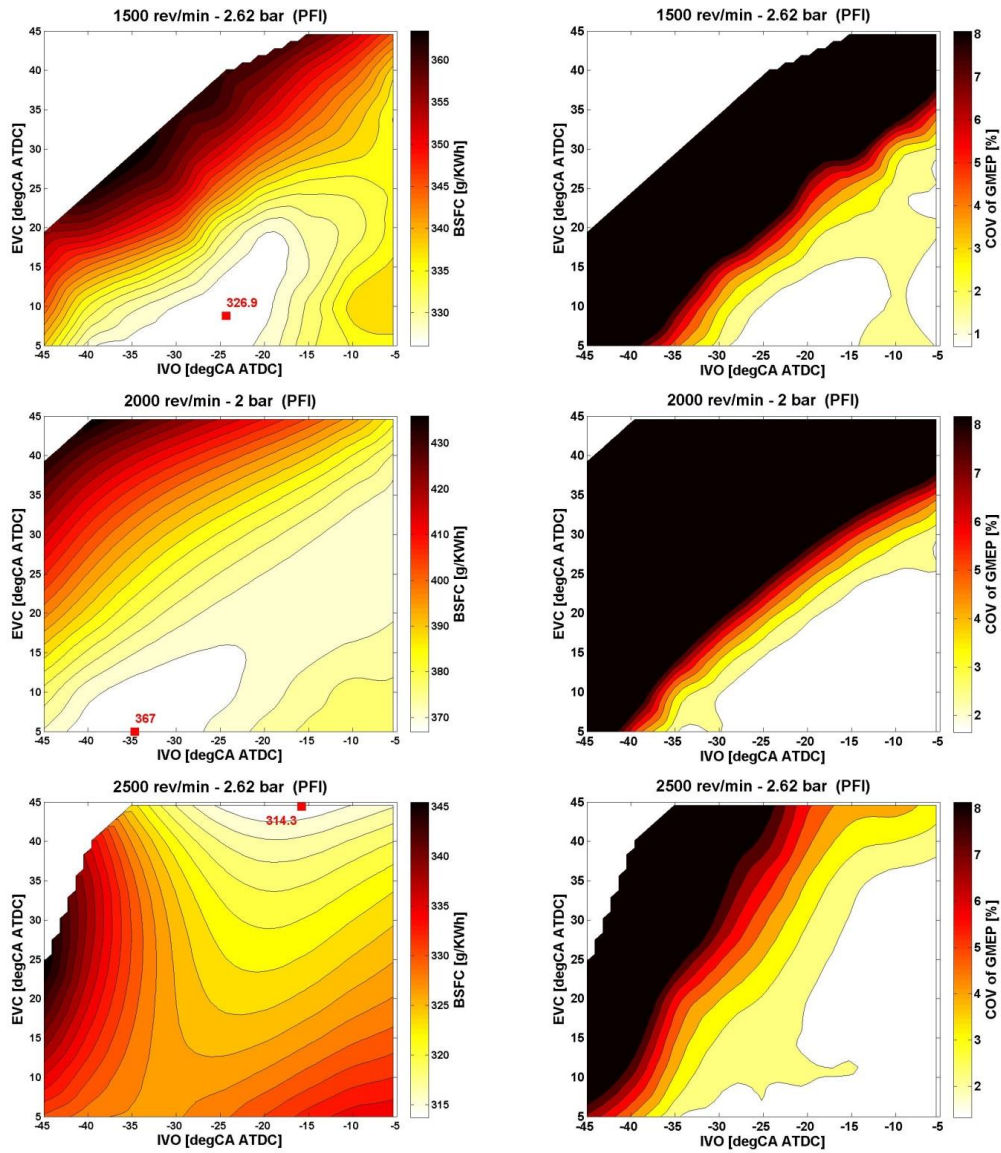
262 **Figure 4.** Contour-plots of BSFC (left) and COV of GMEP (right), as functions of IVO and EVC timing, for the PFI engine (A).  
 263 Operating conditions: engine load of 1 bar (BMEP) and engine speed of 2500 rev/min.



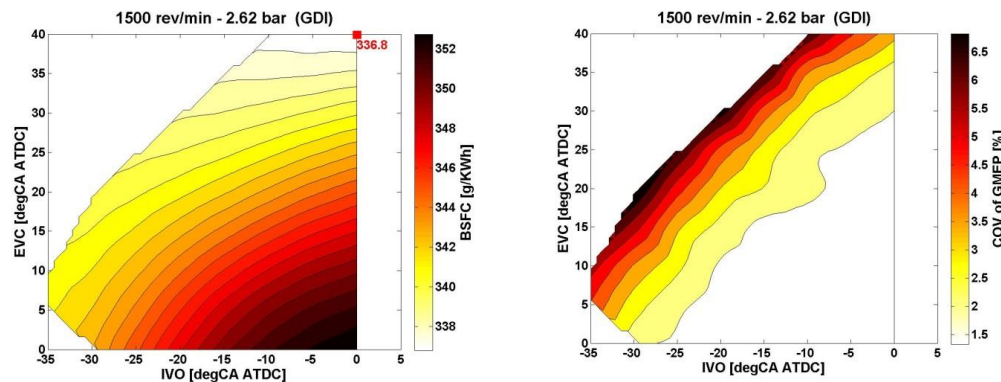
265 **Figure 5.** Contour-plots of BSFC (left) and COV of GMEP (right), as functions of IVO and EVC timing, for the GDI engine (B).  
 266 Operating conditions: engine load of 1 bar (BMEP) and engine speed of 1500 to 2500 rev/min.  
 267

268 The BSFC response metrics for engine A and B, at load of 2 to 2.6 bar BMEP and increasing speed,  
 269 are presented in Figures 6 and 7. The thermal efficiency of engine A, as indicated by the BSFC data,  
 270 appears to be heavily influenced by combustion stability. Figure 4 shows that for engine speed up to  
 271 2000 rev/min, the unsuitably high cycle-by-cycle variability hides the effect of VCT on specific fuel  
 272 consumption. The calculated BSFC minima require early IVO timing (25 to 35 CA deg BTDC), along  
 273 with a moderate delay of the exhaust VCT setting (EVC of 5 to 10 CA deg ATDC). As engine speed  
 274 rises to 2500 rev/min, engine A acquires increased stability and a much wider range of VCT variation  
 275 becomes available; the influence of the VCT setting now assumes similar traits as the 1 bar BMEP  
 276 case. Best engine thermal efficiency is associated to extremely retarded exhaust VCT setting (45 CA  
 277 deg ATDC), in combination with a moderate degree of intake VCT advance (15 CA deg BTDC).  
 278

279 Figure 7 shows that at an engine load of 2 to 2.6 bar BMEP, the BSFC response metrics for engine B  
 280 are significantly similar to the 1 bar BMEP case. At the lower engine speed investigated (1500  
 281 rev/min), IVO for best efficiency continues to be located close to TDC whereas, owing to the  
 282 inherently reduced dilution, optimal exhaust VCT setting is retarded to 35 or 40 CA deg ATDC. Any  
 283 changes to the intake VCT setting determine an unacceptable drop in combustion stability, with the  
 284 COV quickly approaching the 5% threshold. As the engine speed increases, earlier intake VCT  
 285 timings become affordable as expected. Remarkably, Figure 7 shows that, at 2500 rev/min and 2.6  
 286 bar BMEP, any IVO/EVC combination giving valve overlap duration between 50 and 55 CA deg  
 287 ensures about 3.0% BSFC reduction compared to the reference setting (IVO= 5 CA deg BTDC; EVC=  
 288 5 CA deg ATDC). Any larger overlap combination becomes detrimental, most likely due to excessive  
 289 cylinder charge dilution. At these running conditions, the optimal VCT setting is somewhat biased  
 290 towards earlier IVO, rather than later EVC. Such BSFC response, typical of the mid part-load  
 291 envelope as shown in the next section, suggests earlier IVO/IVC setting helps preventing excessive  
 292 fresh-charge back-flow, ultimately increasing the volumetric efficiency.  
 293



294 **Figure 6.** Contour-plots of BSFC (left) and COV of GMEP (right), as functions of IVO and EVC timing, for the PFI engine (A).  
 295 Operating conditions: engine load of 2 to 2.62 bar (BMEP) and engine speed of 1500 to 2500 rev/min.  
 296



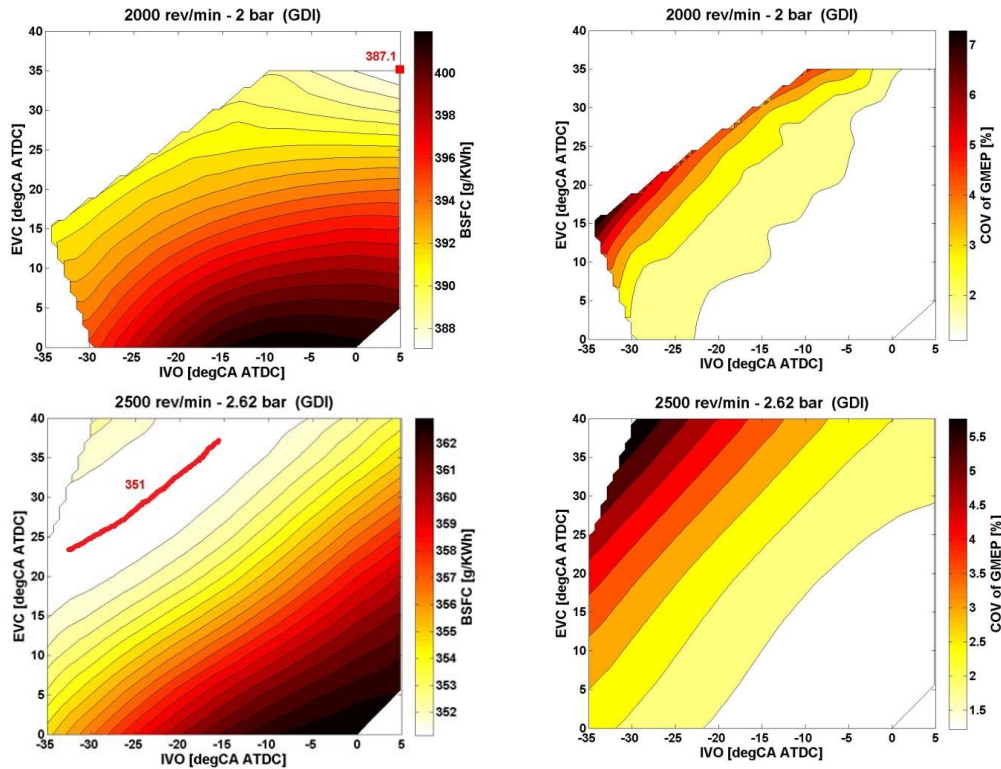
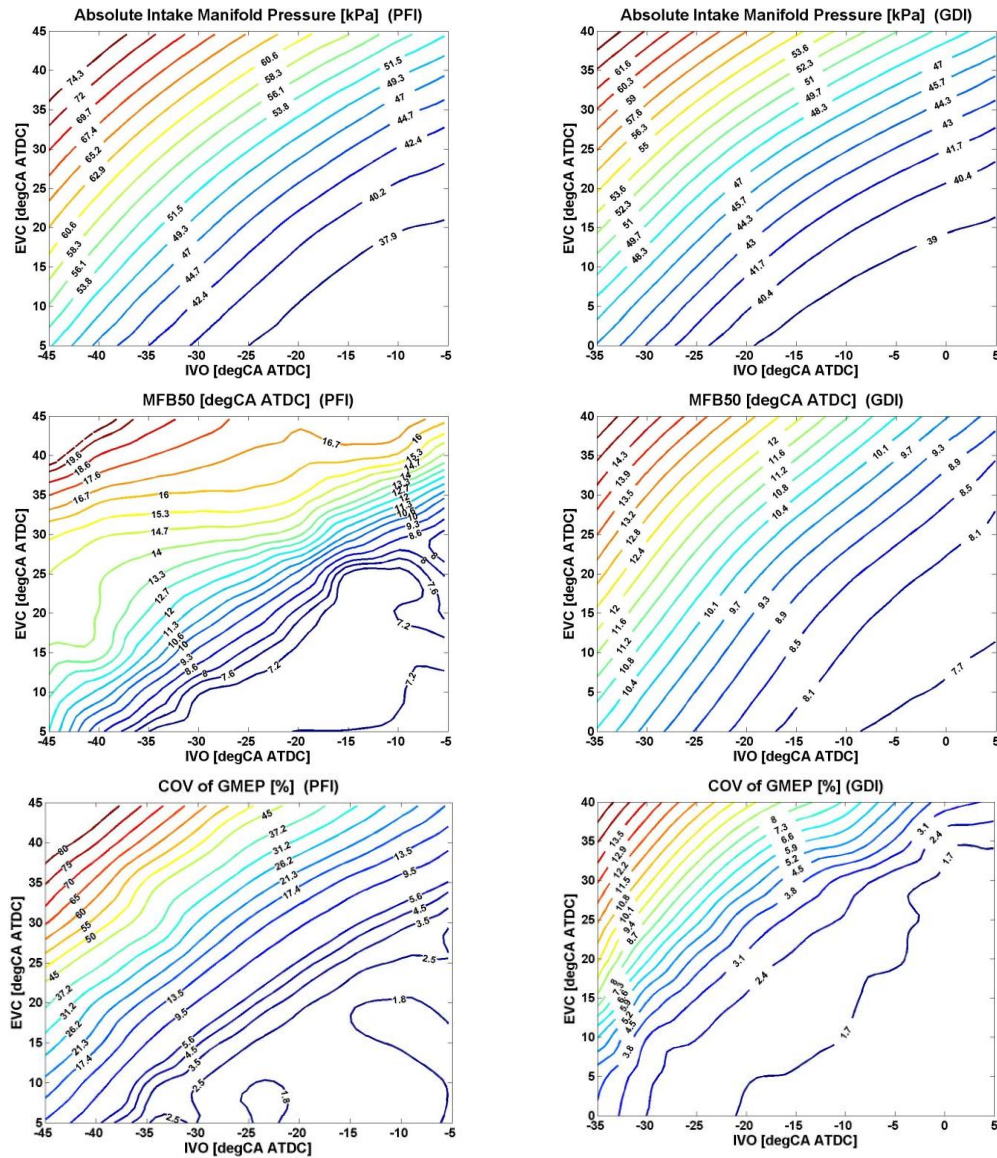


**Figure 7.** Contour-plots of BSFC (left) and COV of GMEP (right), as functions of IVO and EVC timing, for the GDI engine (B). Operating conditions: engine load of 2 to 2.62 bar (BMEP) and engine speed of 1500 to 2500 rev/min.

Figure 8 shows the variation of intake manifold pressure (MAP), MFB50 and, again, COV of GMEP, as a function of the VCT setting, at 2000 rev/min and 2 bar BMEP. These operating conditions were selected as they are representative of the engines' behaviour in the low part-load region. For completeness, data include not only experimental measurements, but also interpolated values to cover the full range of intake and exhaust VCT variation. Supporting data on Pumping Mean Effective Pressure (PMEP) and Indicated engine Torque (IT) are reported in Appendix 1.

Owing to the inherent increase in internal hot gas recirculation, and the consequent need for intake de-throttling, the intake manifold pressure grows with both the degree of IVO advance and the degree of EVC retard. The highest level of intake pressure is consistently associated to the widest symmetrical valve overlap duration. As evident, both MFB50 and COV of GMEP vary in a similar fashion as the intake pressure. Engine A suffers from volumetric efficiency losses, most likely due to the process of port fuel injection; by contrast, the process of direct injection in engine B favours cylinder filling, owing to cylinder charge cooling. At given VCT setting, engine A requires greater manifold pressure to balance a fixed dynamometer torque. In spite of this, the combustion process in engine A quickly degrades with increasing overlap duration, becoming slower and longer (hence, more unstable) as indicated by the MFB50 contour-plots. The latest generation, direct injection system used in engine B ensures a more precise fuel metering per cycle/cylinder, contributing towards increased stability. Figure 8 shows that, for given VCT setting, engine A is much less stable than engine B; in turn, this carries dramatic influence on the selection of an optimal VCT setting for fuel economy.

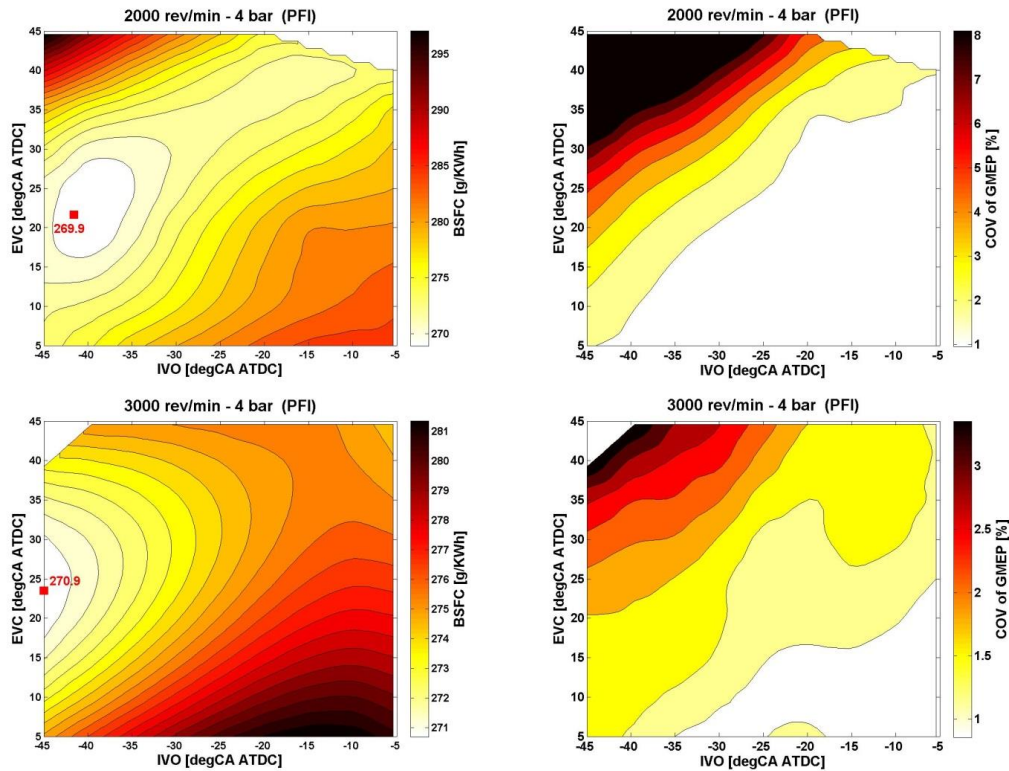


322 **Figure 8.** Contour-plots of intake manifold pressure, location of 50% MFB and COV of GMEP as a function of the VCT setting,  
 323 for engine A (left) and engine B (right). Operating conditions: engine load of 2 bar (BMEP) and engine speed of 2000 rev/min  
 324

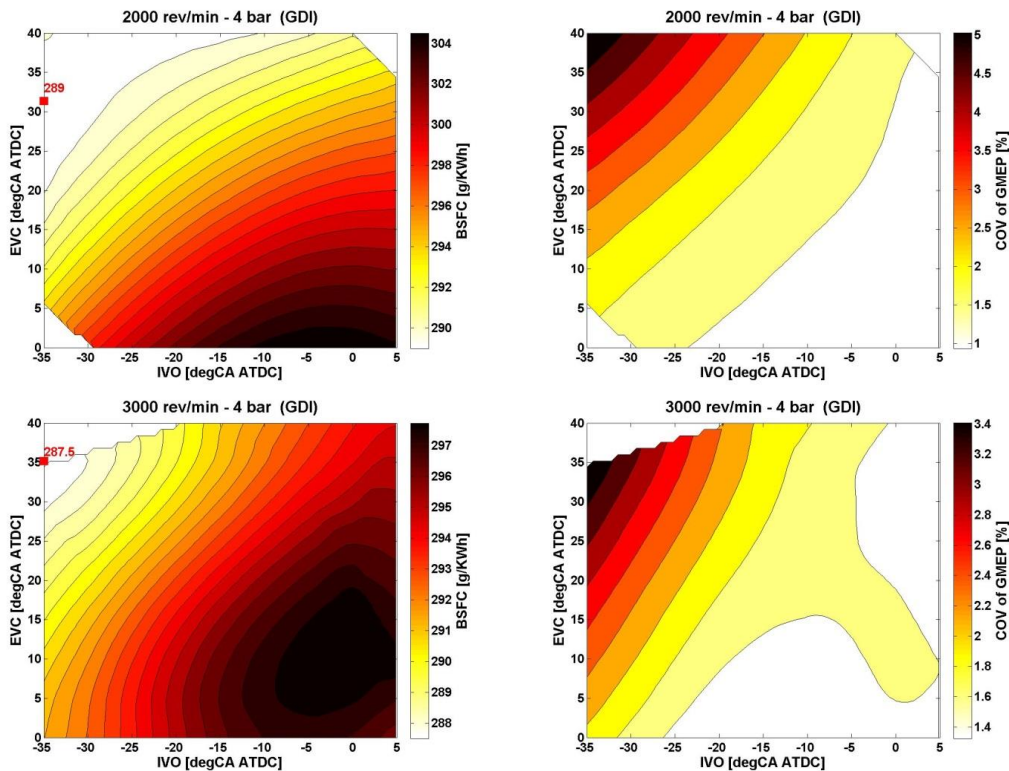
325 **3.2 Influence of VCT setting in the mid part-load region**

326 Figures 9 and 10 show BSFC as a function of intake and exhaust valve timing, at 4 bar BMEP and  
 327 increasing engine speed. With the exception of the top left corner of the 2000 rev/min COV map in  
 328 Figure 9, the measured cyclic variability is well within the 5% threshold, enabling a much more  
 329 consistent behaviour across the two engine platforms. Experimental measurements of internal EGR  
 330 were not performed; nevertheless, at an engine load of 4 bar BMEP and above, both amount and  
 331 variation of in-cylinder charge dilution are expected to be rather limited [8, 9, 14]. This would enable  
 332 the two engines to virtually exploit the full spectra of intake and exhaust VCT variation, with potential  
 333 benefits associated to both early IVC/IVO (greater effective compression ratio; lower pumping losses),  
 334 and late EVO/EVC (greater effective expansion ratio; again, lower pumping losses). The BSFC maps  
 335 for engine A (Figure 9) show that while early IVO is always beneficial, EVC timing in excess of about  
 336 25 CA deg ATDC starts showing a detrimental effect. While stability deterioration may have  
 337 constrained the EVC setting in the lower speed case, late EVC in the higher speed case is likely to  
 338 suffer from a less effective blow-down process. The brake thermal efficiency of engine B, as indicated  
 339 by the BSFC data in Figure 10, grows in a similar fashion with both EVC retard and IVO advance,  
 340 reaching its peak for durations of 65 to 70 CA deg. The experimental data suggest at 4 bar BMEP,

341 intake VCT advance is somewhat more valuable than exhaust VCT retard due to the inherently less  
 342 effective blow-down process.  
 343



344 **Figure 9.** Contour-plots of BSFC (left) and COV of GMEP (right), as functions of IVO and EVC timing, for the PFI engine (A).  
 345 Operating conditions: engine load of 4 bar (BMEP) and engine speed of 2000 to 3000 rev/min.  
 346



347 **Figure 10.** Contour-plots of BSFC (left) and COV of GMEP (right), as functions of IVO and EVC timing, for the GDI engine (B).  
 348 Operating conditions: engine load of 4 bar (BMEP) and engine speed of 2000 to 3000 rev/min.

349  
 350 **3.3 Influence of VCT setting in the high part-load region**

351 The variation of BSFC with changes to intake and exhaust VCT setting, at 5 to 5.5 bar BMEP, is  
 352 presented in Figure 11 for engine A and in Figure 12 for engine B. Only three operating points have  
 353 been shown for brevity and the corresponding COV variations not presented as within the 5% stability  
 354 threshold. In the upper portion of the part-load envelope (5 bar BMEP and above), the different make-  
 355 up of the two engines (namely, nominal compression ratio and fuel injection system) determines a  
 356 very different response to VCT changes. Figure 12 shows that the specific fuel consumption of engine  
 357 B declines with both intake advance and exhaust retard, with lowest levels invariably associated to  
 358 extremely advanced intake VCT setting. With only minor exceptions, engine A performs most  
 359 efficiently when late IVO timings between 10 and 5 CA deg BTDC are employed (Figure 11).  
 360 Consistently to one another, the two engines demonstrate highest fuel consumption for small or  
 361 negative valve overlap duration (bottom-right corner of the BSFC response maps).  
 362

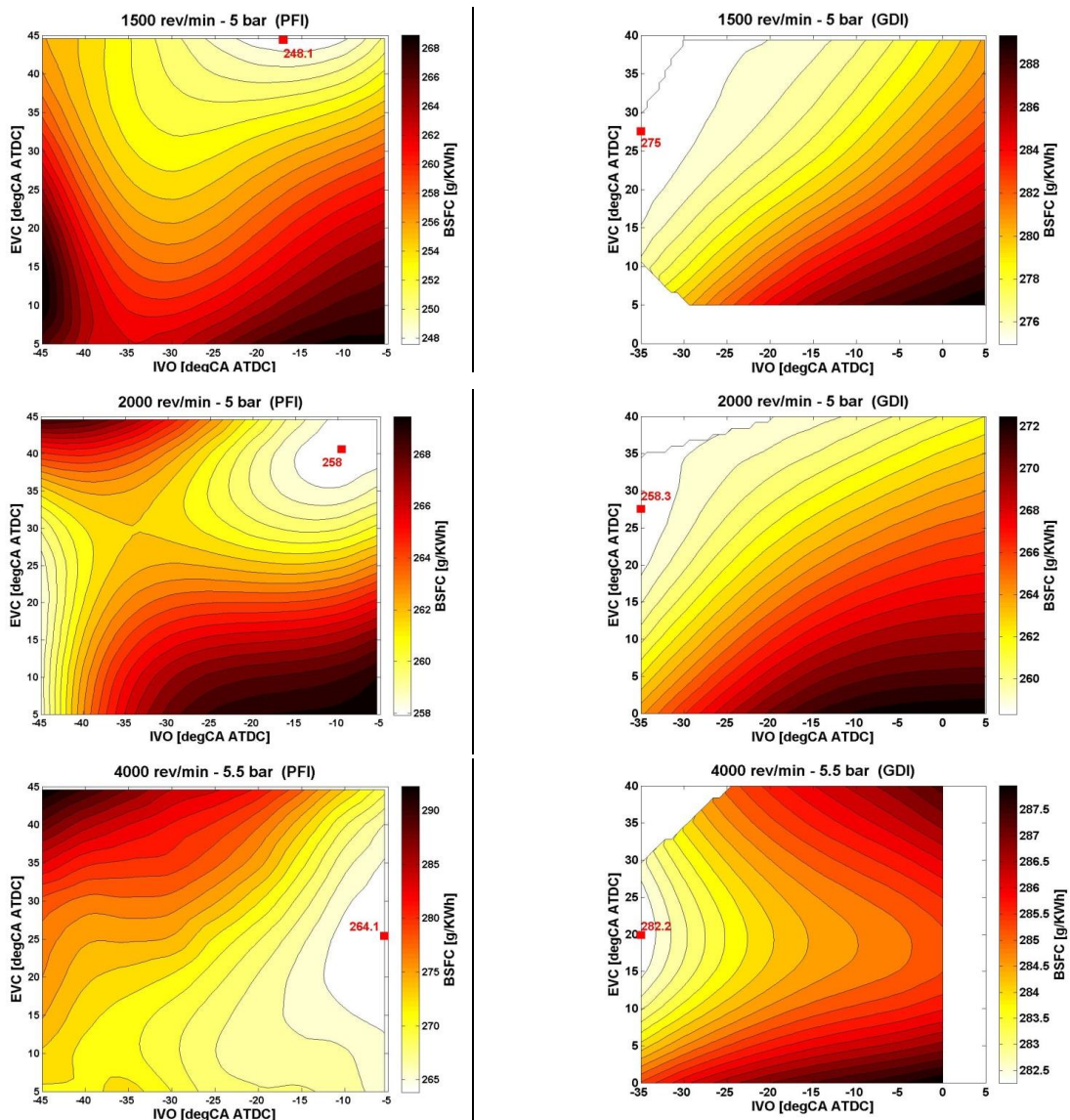
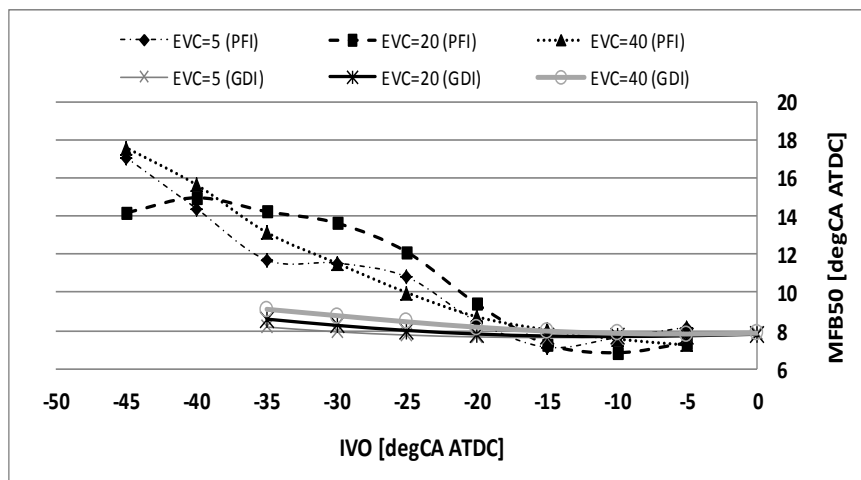


**Figure 11.** Contour-plots of BSFC as a function of IVO and EVC timing, for the PFI engine (A). Operating conditions: engine load of 5 to 5.5 bar (BMEP) and engine speed of 1500 to 4000 rev/min.

**Figure 12.** Contour-plots of BSFC as a function of IVO and EVC timing, for the GDI engine (B). Operating conditions: engine load of 5 to 5.5 bar (BMEP) and engine speed of 1500 to 4000 rev/min.

363  
 364 Engine B features lower nominal compression ratio (10:1) and this enables the implementation of  
 365 early intake VCT setting, without incurring into the inception of knock. The process of fuel direct  
 366 injection also contributes to delaying the occurrence of knock, due to its effect of cylinder charge  
 367 cooling. The absence of a constraint upon the ignition timing allows the use of as early IVO timing as

368 possible, with benefits associated to greater effective compression ratio (more work/cycle), lower  
 369 fresh-charge back-flow (higher volumetric efficiency) and fresh-charge displacement (reduced  
 370 pumping losses). Engine A, which features higher compression ratio (12:1), is knock-limited and  
 371 ignition retardation must be introduced along with advanced intake VCT setting to suppress or delay  
 372 the occurrence of knock. Figure 13 shows the CA location of 50% Mass Fraction Burned for both  
 373 engines at representative operating conditions. The MFB50 is taken as an indication of the ignition  
 374 timing strategy in the upper part-load envelope. As the IVO timing is shifted towards earlier events for  
 375 engine A, the knock-limited MBT ignition strategy shifts combustion further into the expansion stroke,  
 376 with consequent reduction of indicated work per cycle. Compared to engine B, this forces a very  
 377 different response to VCT changes, with greatest efficiency almost invariably associated to late IVO  
 378 operation. As shown in Figure 11, a moderate degree of intake VCT advance (IVO of 15 CA deg  
 379 BTDC) is permitted at 1500 rev/min; the point of minimum BSFC quickly shifts towards later IVO  
 380 events as engine speed increases, owing to an inherently greater knock tendency.  
 381



382  
 383 **Figures 13.** Location of 50% Mass Fraction Burned (MFB50) as a function of IVO timing, at three representative EVC timings.  
 384 The operating conditions, 5 bar BMEP and 1500 rev/min, are indicative of the ignition timing strategy (as represented by the  
 385 combustion process phasing) in the upper part-load envelope of both engines.  
 386

387 The fuel economy response to exhaust VCT changes is consistent across the two engines. The  
 388 comparatively low cylinder charge dilution at these engine loads, allows the two engines to exploit the  
 389 benefits of retarded EVC settings, both in terms of greater energy utilisation (extended power stroke)  
 390 and lower pumping losses. For the PFI engine (A), the retarded intake valve opening enables the use  
 391 of extremely retarded exhaust valve closing (40 to 45 CA deg ATDC), up to an engine speed of 2500  
 392 rev/min. At the highest engine speed investigated (4000 rev/min), lowest BSFC requires overlap  
 393 duration of just 30 CA deg, with limited EVC timing of 25 CA deg ATDC. For the GDI engine (B), the  
 394 advanced IVO setting limits the EVC retard to the range 20 to 27 CA deg ATDC, to minimise the  
 395 losses from the less effective blow-down process.  
 396

397 Figures 14 and 15 show the BSFC response metrics at 7 to 7.5 bar BMEP and increasing engine  
 398 speed. The behaviour demonstrated by the two engines in this load range is mostly consistent to the  
 399 other upper part-load cases shown above. Engine A is knock-limited and lowest BSFC is gained using  
 400 retarded intake VCT setting. Extremely advanced intake valve timing is favourable for the lower  
 401 compression ratio, direct injection engine (B). In both cases, a moderate degree of EVC retard is  
 402 permitted at lower engine speed, but causes blow-down losses at higher speed. Figure 14 shows that  
 403 as engine speed reaches 3000 rev/min at 7.5 bar BMEP, some advancement of the IVO setting is  
 404 advantageous also for engine A. At these operating conditions, lowest BSFC was recorded for EVC  
 405 timing of 18 CA deg ATDC, and IVO timing of 22 CA deg BTDC. At engine speed is increased, the hot  
 406 internal burned gas recirculation reduces [8], likely reducing the final cylinder charge temperature at  
 407 IVC. As a result, the knock tendency also decreases, permitting the use of more advanced IVO  
 408 setting without the need to aggressively retarding the ignition timing.  
 409

410 The overall theoretical fuel-economy Variable Camshaft Timing strategy for engine A and engine B, in  
 411 a simplified graphical form which disregards cases heavily affected by combustion stability, is  
 412 presented in the Conclusions section at the end of this paper.  
 413

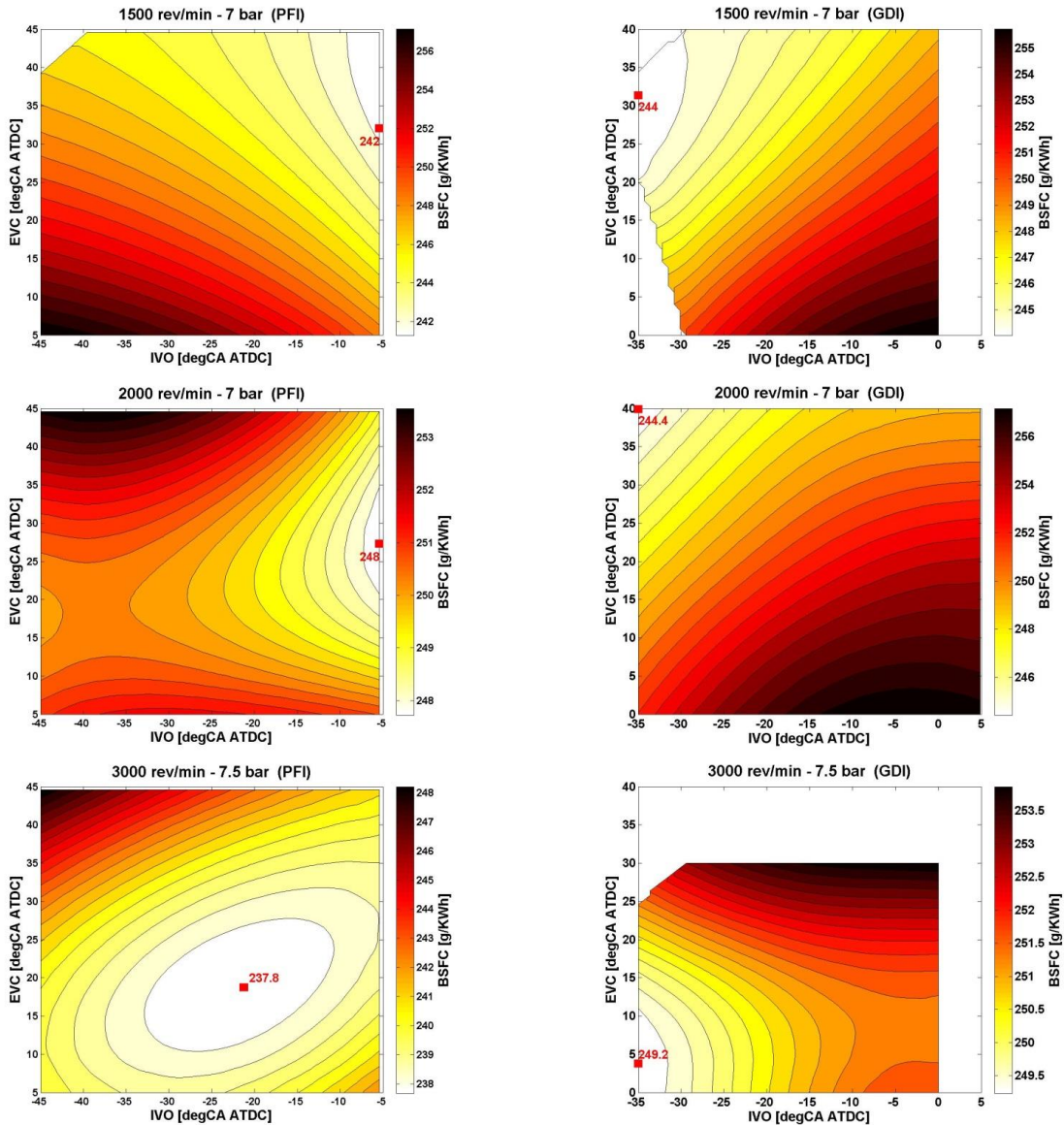


**Figure 14.** Contour-plots of BSFC as a function of IVO and EVC timing, for the PFI engine (A). Operating conditions: engine load of 7 to 7.5 bar (BMEP) and engine speed of 1500 to 3000 rev/min.

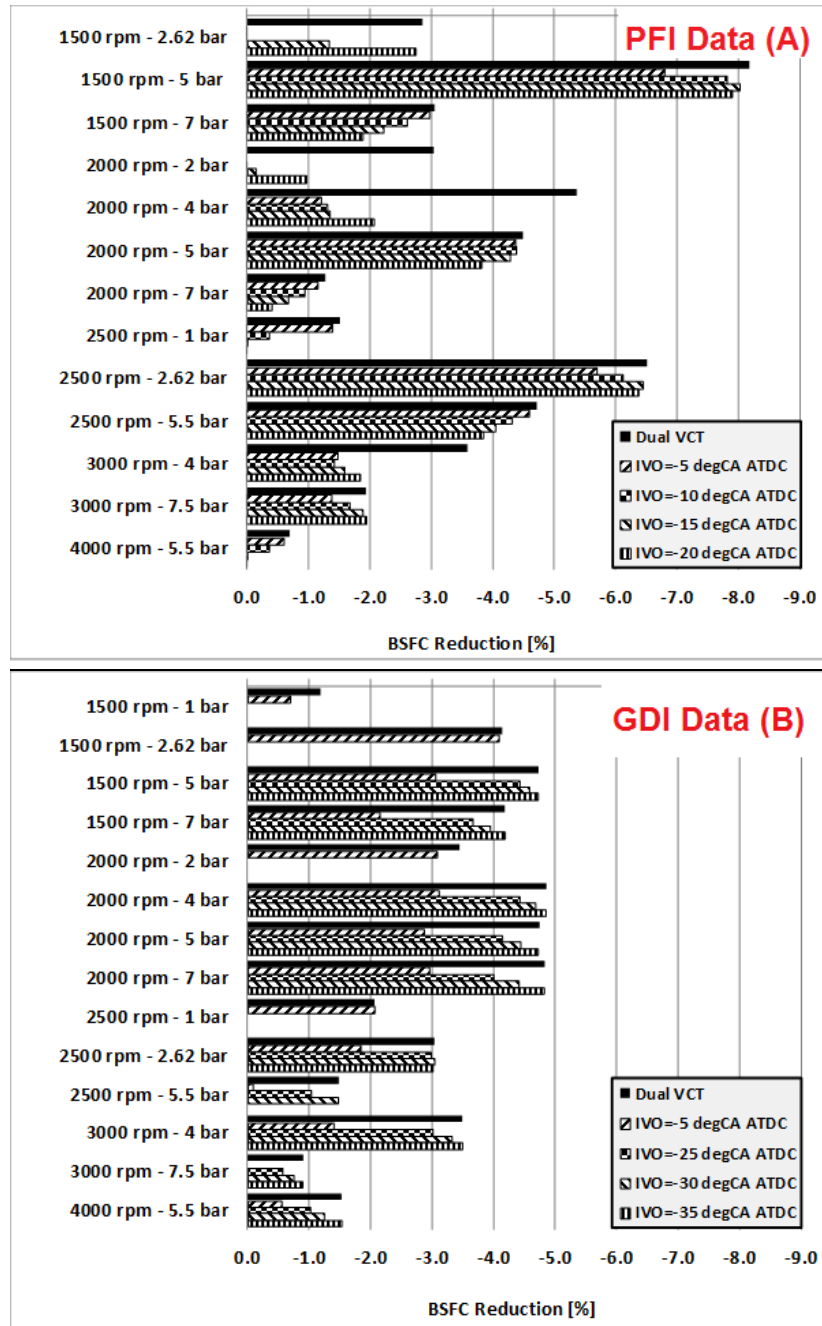
**Figure 15.** Contour-plots of BSFC as a function of IVO and EVC timing, for the GDI engine (B). Operating conditions: engine load of 7 to 7.5 bar (BMEP) and engine speed of 1500 to 3000 rev/min.

414  
 415 **3.4 Overall analysis of fuel economy in the part-load envelope**

416 The analysis presented above shows that as engine speed and load are varied in the part-load  
 417 envelope, changes to both intake and exhaust VCT settings are needed to gain optimal fuel economy.  
 418 Theoretically, both engines would benefit from a dual-independent valve timing strategy.  
 419 Nevertheless, dual-independent systems are more expensive, less practical, and show slower  
 420 response during transient operation when compared to one-variable-camshaft-only approaches. The  
 421 VCT strategy in a specific engine operating range must then carefully consider the trade-off between  
 422 potential fuel savings, and practical deployment of a complicated mechanical system.

423  
 424 Figure 16 summarises the BSFC percent variation between various potential VCT settings and a  
 425 reference setting where IVO= 5 CA deg BTDC and EVC= 5 CA deg ATDC. At each operating  
 426 condition, the “Dual VCT” horizontal bars refer to the best strategy identified above, whereas the other  
 427 bars refer to fixed IVO and best exhaust-only strategies. The choice of IVO settings was dictated by  
 428 the BSFC response metrics examined previously. Some fuel-economy bars are missing as

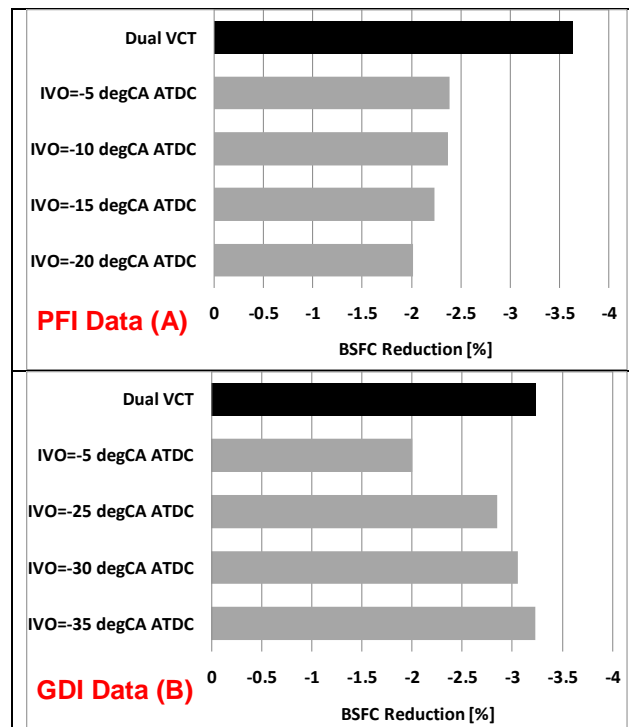
429 experimental records were not available. For both engine platforms, the dual VCT strategy invariably  
 430 enables greatest fuel economy; nevertheless, at some running conditions, specific exhaust-only  
 431 strategies determine very similar benefits. For engine A, the BSFC improvement was in excess of 8%  
 432 at 1500 rev/min and 5 bar BMEP and in excess of 6% at 2500 rev/min and 2.6 bar BMEP. These  
 433 values are in line with those reported recent literature [9, 10, 12, 13]. For the more efficient engine B,  
 434 the improvement associated to using variable valve timing was smaller, but extended to wider ranges  
 435 of running conditions. Compared to the reference VCT setting, BSFC decreased of almost 5% at 1500  
 436 rev/min and engine load between 5 and 7 bar BMEP, and at 2000 rev/min and load between 4 and 7  
 437 bar BMEP.  
 438



439 **Figure 16.** BSFC percent reduction between various VCT settings and reference setting (IVO= 5 CA deg BTDC and EVC= 5  
 440 CA deg ATDC), at all operating conditions investigated. Top plot: PFI engine (A); Bottom plot: GDI engine (B).  
 441

442 The BSFC percent reductions, averaged across all experimental conditions, are presented in Figure  
 443 17. The Dual VCT strategy enables average fuel saving in excess of 3.5% and 3.25% for engine A  
 444 and B, respectively. The best exhaust-only VCT strategy for engine A was based on fixed IVO timing

445 of 5 CA deg BTDC and caused average fuel saving of 2.4%. The best exhaust-only strategy for  
 446 engine B saw IVO timing fixed at 35 CA deg BTDC; the average saving was 3.25%. These results are  
 447 clearly aligned with the previous analysis which showed a knock-limited PFI engine (A), favoured by  
 448 retarded IVO setting; and, by contrast, a lower compression ratio GDI engine (B), favoured by early  
 449 IVO setting.  
 450



451  
 452 **Figure 17.** BSFC percent reduction between various VCT settings and reference setting (IVO= 5 CA deg BTDC and EVC= 5  
 453 CA deg ATDC), averaged upon all operating conditions investigated. Top plot: PFI engine (A); Bottom plot: GDI engine (B).  
 454

455 **4. CONCLUSIONS**

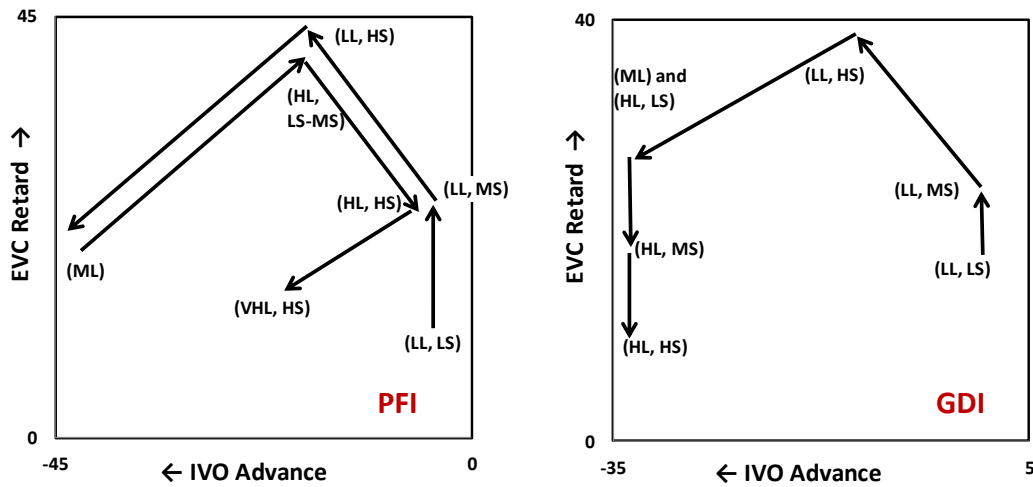
456 Variable camshaft timing strategies have been investigated in two modern, small-capacity, spark  
 457 ignition engines. Both engines featured modern-design, 4-valve/cylinder, pent-roof geometry and  
 458 same displacement volume of 0.333 litre/cylinder. The PFI engine featured higher compression ratio  
 459 of 12:1, whereas the GDI engine featured lower compression ratio of 10:1. The study focused on the  
 460 connection between valve timing setting and fuel economy at part-load operating conditions. The  
 461 study unveiled that engine specifics such as, notably, compression ratio and fuel injection technology,  
 462 have a profound influence upon the VCT strategy which maximises engine thermal efficiency,  
 463 especially in the upper part-load envelope.  
 464

465 The simplified traits of the fuel-economy VCT strategy for the two engines are presented in graphical  
 466 form in Figure 18. At low engine load both engines benefit from retarded IVO timing, which limits the  
 467 cylinder charge dilution and maximise combustion stability. As engine speed increases, increased  
 468 retard of the EVC timing becomes advantageous, most likely because it enables greater effective  
 469 expansion ratio.  
 470

471 At medium engine load, owing to the inherent reduction of internal charge dilution, both engines start  
 472 exploiting the beneficial influence of advanced IVO as well as retarded EVC timing. The experimental  
 473 data suggest that, for both engines but especially for the PFI platform, intake VCT advance is  
 474 somewhat more valuable than exhaust VCT retard due to a less effective blow-down process at this  
 475 engine load.  
 476

477 At the higher loads investigated, the two engines show a very different response to the valve timing  
 478 setting. The lower compression ratio GDI engine continues to benefit from advanced IVO timing,  
 479 whereas the degree of EVC retard must be moderated as engine speed increases to minimise the  
 480 exhaust blow-down losses. As shown in Figure 18, the higher compression ratio PFI engine is knock-  
 481 limited and this forces the VCT strategy to “come back on itself” towards regions of low IVO advance

482 and low hot gas internal recirculation. At the highest load investigated (7.5 bar BMEP), a moderate  
 483 degree of intake advance becomes again favourable as speed increases, owing to reduced hot  
 484 internal dilution and hence reduced knock tendency.  
 485



486 **Figure 18.** Simplified fuel-economy VCT strategy for the two small-size engines at part-load operating conditions. Left plot: PFI  
 487 engine (A); Right plot: GDI engine (B). Arrows describe a path between the low load/low speed and the high load/high speed  
 488 conditions investigated. Legend: LL=Low Load (1-2.6 bar BMEP); ML= Mid Load (4 bar BMEP); HL=High Load (7-7.5 bar  
 489 BMEP); LS=Low Speed (1500 rev/min); MS= Mid Speed (2000-2500 rev/min); HS= High Speed (3000-4000 rev/min); for the  
 490 PFI engine (A), a further condition is identified: VHL= Very High Load (7.5 bar BMEP).  
 491

492 The theoretical best dual-independent VCT strategy determines peak BSFC reduction in excess of  
 493 8% for the PFI engine; maximum reduction was just short of 5% for the more efficient GDI platform.  
 494 The BSFC reduction, averaged upon all part-load operating conditions investigated, was 3.5% for the  
 495 PFI engine, and 3.25% for the GDI one.  
 496

497 For both engine platforms, the upper part-load envelope benefits almost invariably from fixed IVO  
 498 setting. Consequently, specific exhaust-only VCT strategies may be conceived and deployed, which  
 499 enable similar fuel savings as the less practical dual-independent strategy.  
 500

501 **ACKNOWLEDGEMENTS**

502 The Authors wish to thank Ford Motor Company for the provision of experimental data and for the  
 503 permission to publish this paper.  
 504

505 **REFERENCES**

506 [1] International Energy Agency, Policy Pathways: Improving the Fuel Economy of Road Vehicles - A  
 507 policy package, 2011. Available at:  
 508 [http://www.iea.org/publications/freepublications/publication/PP5\\_Fuel\\_Economy\\_FINAL\\_WEB\\_Oct\\_2](http://www.iea.org/publications/freepublications/publication/PP5_Fuel_Economy_FINAL_WEB_Oct_2012.pdf)  
 509 [012.pdf](http://www.iea.org/publications/freepublications/publication/PP5_Fuel_Economy_FINAL_WEB_Oct_2012.pdf)  
 510  
 511 [2] Corvino, C., Calabretta, M., Zanasi, R., Modeling of Variable Valve Timing on High Performance  
 512 Engine using Power-Oriented Graphs Method, SAE Technical Paper 2011-24-0150, 2011  
 513  
 514 [3] Taylor, J., Fraser, N., Dingelstadt, R., Hoffmann, H., Benefits of Late Inlet Valve Timing Strategies  
 515 Afforded Through the Use of Intake Cam In Cam Applied to a Gasoline Turbocharged Downsized  
 516 Engine, SAE Technical Paper 2011-01-0360, 2011  
 517  
 518 [4] Turner, J. W. G., Pearson, R.J., The turbocharged direct-injection spark-ignition engine, in Zhao H.  
 519 (ed.), Direct injection combustion engines for automotive applications: Science and Technology. Part  
 520 1: spark-ignition engines, ISBN 1-84567-389-2, Woodhead Publishing Limited: Cambridge, 2009  
 521

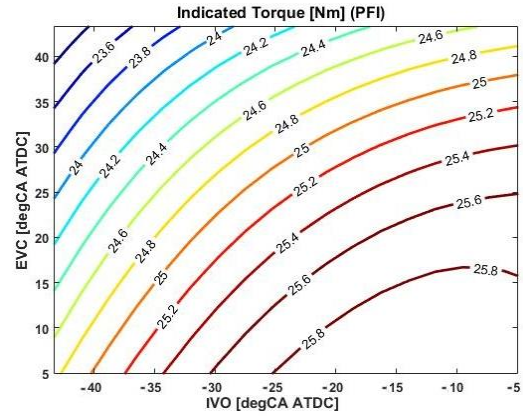
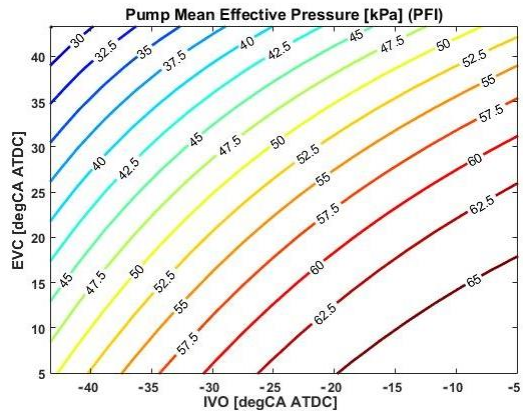
- 522 [5] Shayler, P. J. and Alger, L. C., Experimental Investigations of Intake and Exhaust Valve Timing  
523 Effects on Charge Dilution by Residuals, Fuel Consumption and Emissions at Part Load, SAE paper  
524 2007-01-0478, 2007  
525
- 526 [6] Bonatesta, F., Premixed combustion in spark ignition engines and the influence of operating  
527 variables, book chapter. In: Ng HK (Ed.), Advances in internal combustion engines and fuel  
528 technologies, ISBN: 978-953-51-1048-4, In-Tech, 2013.  
529
- 530 [7] Gray, C., A Review of Variable Engine Valve Timing, SAE Technical Paper 880386, 1988  
531
- 532 [8] Bonatesta, F., Shayler, P. J., Factors influencing the burn rate characteristics of a spark ignition  
533 engine with variable valve timing, Proc. Inst. Mech. Eng. Part D: J. Automob. Eng., 222: 2147–2158,  
534 2008  
535
- 536 [9] Fontana, G., Galloni, E., Palmaccio, R. and Torella, E., The Influence of Variable Valve Timing on  
537 the Combustion Process of a Small Spark-Ignited Engine, SAE Technical Paper 2006-01-0445, 2006  
538
- 539 [10] Cairns, A., Todd, A., Hoffman, H., Aleiferis, P., Malcolm, J., Combining Unthrottled Operation with  
540 Internal EGR Under Port and Central Direct Fuel Injection Conditions in a Single Cylinder SI Engine,  
541 SAE Technical Paper 2009-01-1835, 2009  
542
- 543 [11] Heywood, J. B., Internal Combustion Engine Fundamentals. McGraw Hill, Automotive  
544 Technology Series, 1988  
545
- 546 [12] Tuttle, J., Controlling Engine Load by means of Early Intake Valve Closing, SAE Technical Paper  
547 820408, 1982  
548
- 549 [13] Lenz, H., Wichart, K. Gruden, D., Variable Valve Timing – A Possibility to Control Engine Load  
550 without Throttle, SAE Technical Paper 880388, 1988  
551
- 552 [14] Leone, T. G., Christenson, E., Stein, R., Comparison of Variable Camshaft Timing Strategies at  
553 Part Load, SAE Technical Paper 960584, 1996  
554
- 555 [15] Kramer, U., Philips, P., Phasing Strategy for an Engine with Twin Variable Cam Timing, SAE  
556 Technical Paper 2002-01-1101, 2002  
557
- 558 [16] Fraser, N., Blaxill, H., Lumsden, G., Bassett, M., Challenges for Increased Efficiency through  
559 Gasoline Engine Downsizing, SAE Technical Paper 2009-01-1053, 2009  
560
- 561 [17] Lecointe, B., Monnier, G., Downsizing a Gasoline Engine using Turbocharging with Direct  
562 Injection, SAE Technical Paper 2003-01-0542, 2003  
563
- 564 [18] McAllister, M. J., Buckley, D. J., Future gasoline engine downsizing technologies - CO2  
565 improvements and engine design considerations, Institution of Mechanical Engineers, Internal  
566 Combustion Engines Conference, London, December 2009 (Paper number C684/018)  
567
- 568 [19] Kasseris, E. P., Heywood, J. B., Comparative Analysis of Automotive Powertrain Choices for the  
569 next 25 years, SAE Technical Paper 2007-01-1605, 2007  
570
- 571 [20] Shinagawa, T., Kudo, M., Matsubara, W., Kawai, T., The New Toyota 1.2-Liter ESTEC  
572 Turbocharged Direct Injection Gasoline Engine, SAE Technical Paper 2015-01-1268, 2015  
573
- 574 [21] Krebs, R., Szengel, R., Middendorf, H., Sperling, H., et Al., The New Dual-Charged FSI Petrol  
575 Engine by Volkswagen Part 2: Thermodynamics, MTZ 12/2005, 66: 23-26, 2005  
576
- 577 [22] Turner, J., Popplewell, A., Patel, R., Johnson, T. et Al., Ultra Boost for Economy: Extending the  
578 Limits of Extreme Engine Downsizing, SAE Int. J. Engines 7(1):387-417, 2014  
579

- 580 [23] Police, G., Diana, S., Giglio, V., Iorio, B., Rispoli, N., Downsizing of SI Engines by Turbo-  
581 Charging, 8th Biennial ASME Conference on Engineering Systems Design and Analysis, Turin, Italy,  
582 July 2006  
583
- 584 [24] Wirth, M., Mayerhofer, U., Piock, W. F., Fraidl, G. K., Turbocharging the DI Gasoline Engine, SAE  
585 Technical Paper 2000-01-0251, 2000  
586
- 587 [25] Baêta, J. G. C., Pontoppidan, M., Silva, T. R., Exploring the limits of a down-sized ethanol direct  
588 injection spark ignited engine in different configurations in order to replace high-displacement gasoline  
589 engines, Energy Conversion and Management, 105: 858-871, 2015.  
590
- 591 [26] Li, Y., Zhao, H., Stansfield, P., Freeland, P., Synergy between Boost and Valve Timings in a  
592 Highly Boosted Direct Injection Gasoline Engine Operating with Miller Cycle, SAE Technical Paper  
593 2015-01-1262, 2015  
594
- 595 [27] Birckett, A., Engineer, N., Arlauskas, P., Shirley, M. et Al., Mechanically Supercharged 2.4L GDI  
596 Engine for Improved Fuel Economy and Low Speed Torque Improvement, SAE Technical Paper  
597 2014-01-1186, 2014  
598
- 599 [28] Delphi Powertrain Systems, Gasoline Engine Management Systems, Delphi Variable Cam  
600 Phaser, 2015. Available at: <http://www.delphi.com/manufacturers/auto/powertrain/gas/valvetrain/vcp>  
601
- 602 [29] Barlow, T. J., Latham, S., McRae, I. S., Boulter, P.G., A reference book of driving cycle for use in  
603 the measurement of road vehicle emissions (Version 3), Published Project Report PPR354, 2009  
604
- 605 [30] Brunt, M. F. J., Emtage, A. L., Evaluation of IMEP routines and analysis errors, SAE Technical  
606 Paper 960609, 1996  
607
- 608 [31] Brown, N. M., Characterisation of Emissions and Combustion Stability of a Port Fuelled Spark  
609 Ignition Engine, PhD Thesis, University of Nottingham, 2009  
610
- 611 [32] Cary, M., A Model Based Engine Calibration Methodology for a Port Fuel Injection, Spark-Ignition  
612 Engine, PhD Thesis, University of Bradford, 2003  
613
- 614 [33] Booker, A. J., Design and Analysis of Computer Experiments, 7<sup>th</sup> AIAA/USAF/NASA/ISSMO  
615 Symposium on Multidisciplinary Analysis & Optimization, St. Louis, MO, AIAA, 1, 118-128, AIAA-98-  
616 4757, 1998  
617

## 618 **APPENDIX 1**

619 This section reports data of Pumping Mean Effective Pressure (PMEP) and Indicated Engine Torque  
620 (IT) as a function of intake and exhaust valve timing. Figure A1.1 shows the corresponding contour-  
621 plots for engine A (PFI) at engine load of 2 bar (BMEP) and engine speed of 2000 rev/min. As  
622 anticipated in section 3.1, the operating conditions have been selected as they illustrate the engine  
623 response which is typical of the lower part-load running envelope. The response of the GDI platform  
624 (engine B) in this region was found to be very similar. The data shown in Figure A1.1 include  
625 interpolated values to cover the full range of intake and exhaust valve timing variability.  
626

627 Referring back to Figure 8, the PMEP shows as expected a strong degree of inverse correlation with  
628 intake manifold pressure (MAP). As the valve overlap is increased, the intake de-throttling needed to  
629 maintain constant engine brake load, induces higher intake manifold pressure; in turn, this lowers the  
630 pumping work and hence the PMEP. While MAP increases, the PMEP is seen to decrease in equal  
631 manner with both the degree of IVO advance and the degree of EVC retard. As shown in Figure A1.1,  
632 the changes in pumping work are reflected by those in indicated torque, which tends to reduce with  
633 increasing symmetric valve overlap to maintain constant brake load.  
634



635  
636  
637  
638

**Figure A1.1.** Contour-plots of Pressure Mean Effective Pressure and Indicated Torque as a function of the VCT setting for engine A (PFI). Operating conditions: engine load of 2 bar (BMEP) and engine speed of 2000 rev/min.